Original paper

Stalactitic rhodochrosite from the 25 de Mayo and Nueve veins, Capillitas, Catamarca, Argentina: Physical and chemical variations

María Florencia MÁRQUEZ-ZAVALÍA[1,2*], James R. CRAIG[3]

[1] *IANIGLA, CCT-Mendoza (CONICET), Avda. A. Ruiz Leal s/n, Parque San Martin, CC330, (5500) Mendoza, Argentina; mzavalia@mendoza-conicet.gov.ar*
[2] *Mineralogía y Petrología, FAD, Universidad Nacional de Cuyo, Centro Universitario, (5502) Mendoza, Argentina*
[3] *Department of Geological Sciences, Virginia Tech, Blacksburg, Virginia, 24061*
[*] *Corresponding author*

Capillitas is an epithermal vein-type deposit in Argentina known for its mineralogical diversity, with more than one hundred and twenty described minerals, including five new species, and for the presence of banded and stalactitic rhodochrosite. Stalactites occur as single or combined cylinders of different sizes, from a few cm to 1.36 m in length and diameters up to 8 cm. Their cross-sections may show diverse aspects: from simple concentric banding to more intricate textures, whereas their external surface can be smooth, with undulations or with a poker-chip-like texture. The color of the stalactites varies from white to raspberry pink, with occasional brown bands toward the edges corresponding to a variety of rhodochrosite called "capillitite". The contents of MnO range from 27.50 to 61.71 wt. % as it may be significantly replaced by CaO, FeO, ZnO and MgO. Replacements are reflected in the various shades of pink and brown displayed by this mineral. The different substitutions in the pink specimens exert only a minor influence on the unit cell parameters, whereas, in the brown variety, their size is significantly smaller with average values for pink rhodochrosite (n = 24): a 4.776 Å, c 15.690 Å and a cell volume of 310.3 Å^3, whereas, "capillitite" unit-cell parameters (n = 7) are: a = 4.739, c = 15.558 with a unit-cell volume of 302.6 Å^3. Conditions of formation of the banded rhodochrosite of the 25 de Mayo vein, obtained from fluid inclusions data, indicate temperatures of 145 ° to 150 °C and salinities of up to 4 wt. % NaCl(eq). The formation of the stalactites is explained by the infiltration of epithermal aqueous liquid, oversaturated with Mn and bicarbonate, into a transiently vapor-filled, isolated cavity.

Keywords: rhodochrosite, stalactites, epithermal deposit, Capillitas, Argentina
Received: 25 January 2022; accepted: 20 May 2022; handling editor: J. Sejkora

1. Introduction

Capillitas, located in Catamarca province in northwestern Argentina (27°20'30"S and 66°23'00"W, Fig. 1), is an intermediate sulfidation, epithermal precious- and base-metal vein deposit hosted in granitic and volcanic rocks. It is located on the eastern slope of the Sierra de Capillitas, in the Sierras Pampeanas region of Catamarca province. The Sierra de Capillitas, with a NE–SW orientation and an extension of 15 km long by 5 km wide, consists of a faulted basement block, limited by two reverse faults: Lavadero to the northwest and El Tigre to the southwest. Angelelli and Rayces (1946) have already indicated that the mineralized veins and dikes are controlled by a joint system in the granite, which follows the NE–SW and NW–SE regional pattern with slight local deviations. The Capillitas deposit is genetically linked to the other mineralization deposits of the Miocene Farallón Negro Volcanic Complex (Márquez-Zavalía and Heinrich 2016, and references therein).

The lithostratigraphy of the area consists of a Paleozoic granite basement, the Capillitas granite, and three minor Cenozoic units: the El Morterito Formation, the Volcanic Complex, and Quaternary deposits. In Capillitas the rocks of the Volcanic Complex form an ellipsoidal diatreme of about 1500 m long by 900 m wide. The most representative lithologies are: rhyolite, brecciated rhyolite, rhyolitic and granitic breccias, dacite porphyry, and trachytic and basaltic dikes. Nineteen veins hosted in granite and volcanic rocks were recognized; they are lenticular to tabular, linear, bent, or sinuous, showing a pinch and swell structure and rough symmetrical banding, with an average thickness of 50 to 70 cm. More than one hundred and twenty minerals were identified in these veins, including five new species: putzite, catamarcaite, ishiharaite, lislkirchnerite and omariniite (Márquez-Zavalía et al. 2020, and references therein) and a variety of brown rhodochrosite: "capillitite" (Galloni 1950). The most abundant species correspond to sulfides and sulfosalts of Cu, Fe, Pb, Zn, As and Sb ± Au, Ag, Bi, Sn and Te, with rhodochrosite and minor quartz as the main gangue minerals (Márquez-Zavalía 1988, 1999; Márquez-Zavalía and Craig 2004; Putz et al. 2009; Márquez-Zavalía et al. 2014).

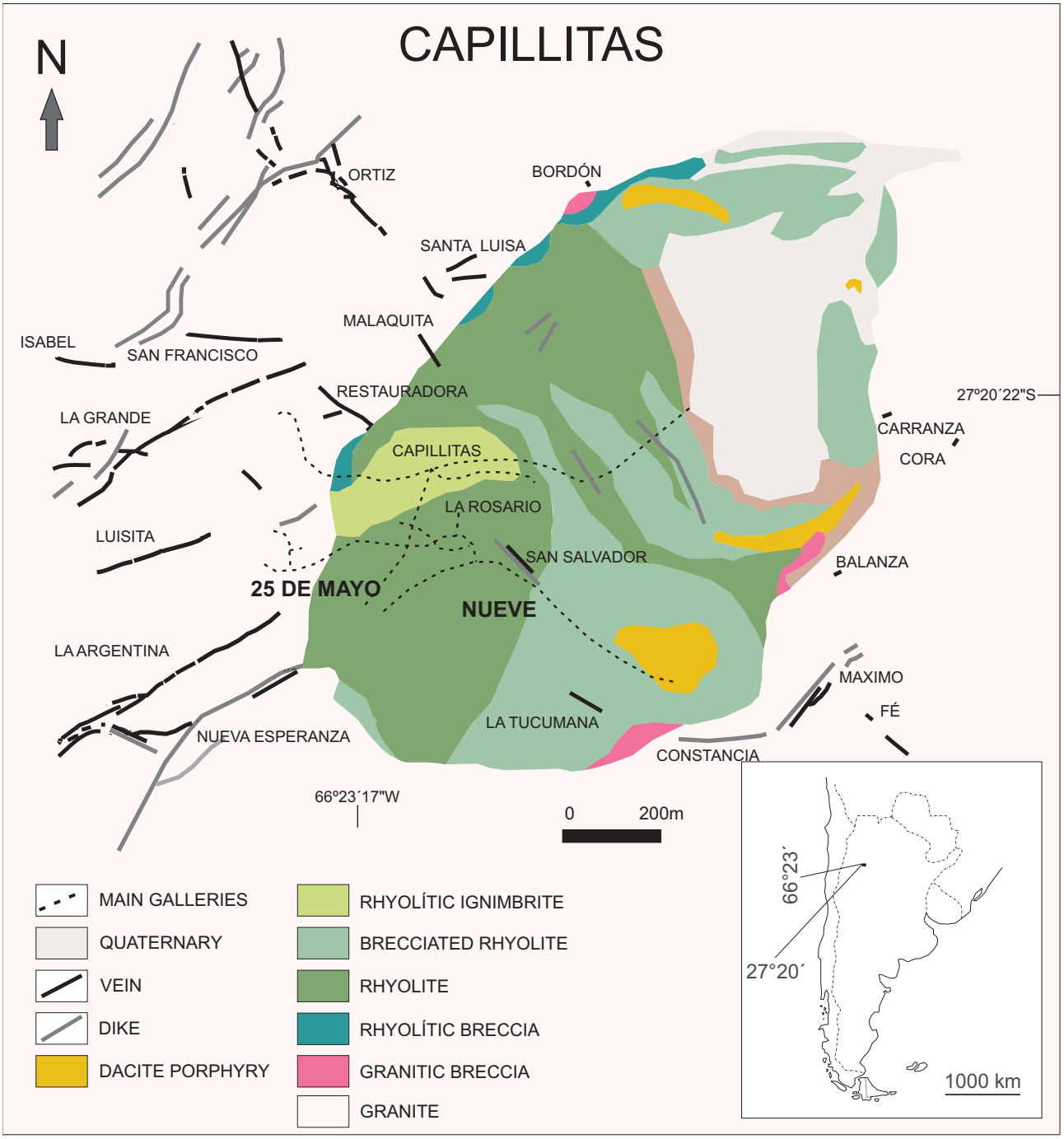

Fig. 1 Schematic geology of Capillitas, showing the location of 25 de Mayo and Nueve veins (modified from Márquez-Zavalía et al. 2020).

The rhodochrosite from Capillitas, also known as Rosa del Inca, is Argentina's national mineral (Márquez-Zavalía 2008). Although it is a relatively frequent species, rhodochrosite from Capillitas is known worldwide for its exceptional stalactitic structure and for the beauty of its banded textures. Although this mineral is widely distributed in the deposit, the cavities with stalactites are quite scarce since they were only found on two occasions. Previous authors (e.g., Radice 1949; Shaub 1972; Angelelli et al. 1974; Brodtkorb and Brodtkorb 1979) mentioned or described the finding prior to 1949, but they did not provide precise data on their location or any *in situ* descriptions of the occurrences. In 1985–86, two cavities were found in the 25 de Mayo vein and some stalactites were also recovered in a nearby sector, corresponding to the Nueve vein (Eng. F. Álvarez pers. commun. 2000; Lieber 2000; Márquez-Zavalía 2008; Behnke 2016).

In this contribution, focused on the 1985–86 find, we present a combination of mineralogical observations, results of electron microprobe analyses (EMPA) and X-ray diffraction data in an attempt to provide insight into the second find of these unusual stalactites.

2. Samples and methodology

Representative samples from the different presentations of the stalactitic rhodochrosite from the two caves found in 1985–86 in the 25 de Mayo vein were selected for this study; twenty polished sections were immersed in Araldite epoxy resin and conventionally prepared and polished for optical examination and electron-microprobe analyses (EMPA). A total of 2744 chemical analyses were carried out in seven traverses on three representative samples of stalactitic rhodochrosite and one of a helictite sample; in addition, 582 analyses were performed along a traverse across a banded pink and brown specimen of rhodochrosite sampled from the ceiling of the main cave. All analyses were carried out with a Cameca SX–50 electron microprobe, in the wavelength dispersion mode, at the Department of Geological Sciences, Virginia Polytechnic Institute and State University, Blacksburg, Virginia, USA. The gaps with no data along the traverses correspond to epoxy intervals. The operating conditions included an accelerating voltage of 15 kV, a sample current of 20 nA and a beam diameter of 2 μm; the counting time was of 20 s for Co and 10 s for the rest of the elements and half of those times for each background. The used standards and analytical lines were as follows: Mg, Ca ($MgCaSi_2O_6$, K_α), Mn (MnO_2, K_α), Fe (FeS_2, K_α), Co ((Co,Ni)As_3, K_α), S, Zn (ZnS, K_α), Sr ($SrTiO_3$, L_α), Cd ($CdWO_4$, L_α) and Ba ($BaSO_2$, L_α). The amount of CO_2 was determined by stoichiometry. The data were reduced using the PAP routine (Pouchou and Pichoir 1985).

Twenty individual bands from seven representative stalactites and seven bands from banded brown rhodochrosite were selected for X-ray powder-diffraction data. These were obtained with a Philips 1710 automated powder diffractometer using monochromatic Cu K_α radiation (λ 1.54060Å) at the Department of Geological Sciences, University of Manitoba, Winnipeg, Canada. For comparative purposes, five non-stalactitic samples of rhodochrosite were included. The data were collected from 10° to 70° 2θ, at a speed of 0.6° per minute. We used Si 640B as an internal standard, and the intensities were observed at peak maxima. Indexing and refinement of the unit-cell dimensions were made using a PC-modified version of the Appleman & Evans (1973) program; we assigned unit weight for each measurement.

3. Results

3.1. Occurrence and description of the stalactites

The most important find of stalactitic rhodochrosite in Capillitas occurred in July 1985, in the 25 de Mayo vein (level –12 m), a few months later, in 1986, at the –8 m level of the same vein, a smaller cavity with more stalactites was found (Eng. F. Álvarez, pers. commun. 2000). The average size of the larger cavity was about 4 m high, 8 m long and 1.5 to 2 m wide. The smallest cavity, discovered in 1986, was 35 cm high, 80 cm long and 30 cm wide. There, several relatively small fragments of stalactite were found on the floor of the cavity. On the ceiling, along with some stalactites, thin, twisted stalactite-like formations -helictites- hang in various directions, in some cases almost horizontally, including several that were bent at diverse angles. Only poor photographic records remain of these findings (Fig. 2) and none of the *in situ* occurrences of the helictites. Five tons of individual, single feeder stalactites and about 16 tons of composite stalactites were recovered. In addition, a few stalagmites up to 5 cm tall and 2.5 cm in diameter were found. A disk of 10 cm wide and 3 cm tall attached to the floor of a cavity that apparently contained no stalactites have been reported by miners; no columns were seen. In 1986, some stalactites were found at level –14, of the Nueve vein. This cavity is located in the vicinity of the 25 de Mayo vein (Fig. 1), although neither the exact location nor the quantity of the recovered material was reliably recorded. In the three locations, veins of banded rhodochrosite were observed on the ceiling of the cavities. After all the stalactites were removed, pumping activities were deactivated in the area and those levels were flooded; to our knowledge, such cavities were not found subsequently.

In the literature, there are four previous references mentioning the first find of stalactitic rhodochrosite from Capillitas. Radice (1949) described the stalactites that are part of the Museo de La Plata collection (Buenos Aires, Argentina), and also mentioned that Franz Mansfeld, in a book published in 1943 and long out of print (as cited in Radice 1949), presented illustrations of the stalactites, but without mention of their *in situ* occurrence. Shaub (1972) reported the existence of stalactites of rhodochrosite from Capillitas and, although he does not provide detailed information on their occurrence, he described a sample and included a photograph. Angelelli et al. (1974) described samples of stalactitic rhodochrosite and mentioned that they came from the 25 de Mayo vein, in a place that could not be visited because it had been abandoned for a long time. However, a miner told them that the cave that contained the stalactites was 6 m long

and 10 m high and that most of the stalactites were lying in pieces on the ground. Brodtkorb and Brodtkorb (1979) showed a thin section of a stalactite and provided results of three chemical analyses corresponding to one brown and two pink bands of the specimen; there is no precise description of the stalactites or the location of the sample within the deposit. No further scientific information has been found on these pre-1980s finds, although fragments of these samples are part of numerous museums and private collections around the world. All the information we provide below was obtained from samples of the 1985–86 findings.

The stalactites hang vertically from the ceiling of the cavities and their size varies greatly, from a few millimeters wide and a few centimeters long to a maximum of 8 cm wide and 1.36 m long. According to the miners, the best stalactites were found where the wall rock is granitic, whereas, in the sectors with rocks of rhyolitic composition, the stalactites were scarce and of poor quality.

The shape of the stalactites is highly variable, from individual cylinders with a symmetrically-centered internal channel (Figs 2b, d, and 3a, b, e) to stalactites that, at some point of their development and being very close to each other, were surrounded by successive layers of growth giving rise to a single larger stalactite with several feeders (Fig. 3c, d). Most of the stalactites consist of concentric layers of variable thickness, generally ranging from a few micrometers to a few millimeters. At first sight, they appear to be separated from each other by clean boundaries (Fig. 3c, e), but under the microscope, they reveal irregularities between the layers (Fig. 3b, d, f), with frequent crenulated boundaries, which in some cases are delimited by crystal faces, especially in the outermost layers.

Scattered crystals of pyrite are generally seen toward the external rim of the stalactites; they are commonly zoned and follow the pattern of the host layers (Fig. 3g). In some cases, pyrite is arranged in bands, generally discontinuous and irregular, reaching up to 1 mm thick and following the outline of the rhodochrosite crystals (Fig. 3h); pyrite is partially

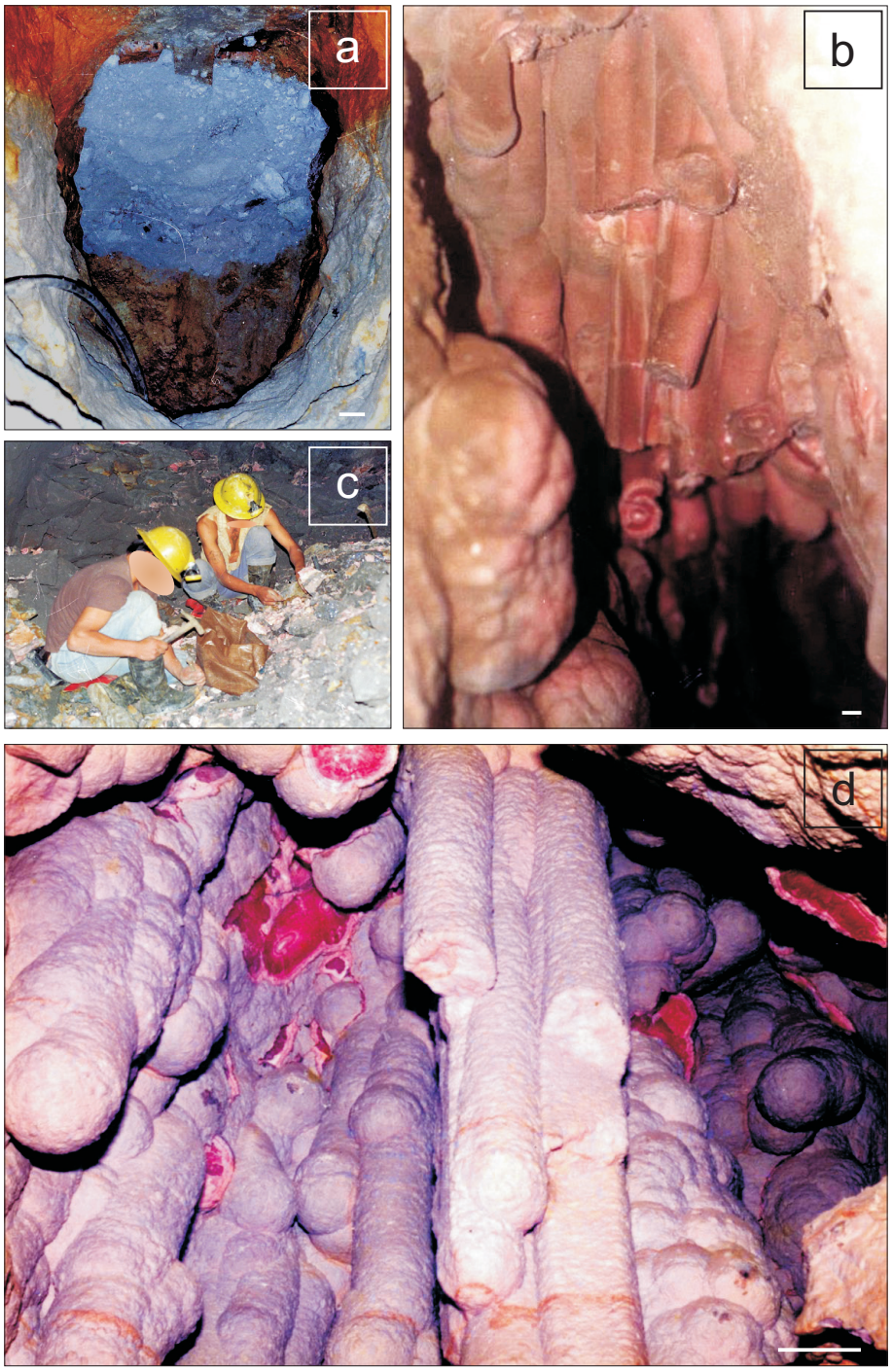

Fig. 2a – Entrance to the bigger cavity. **b** – Partial view of the cavity with stalactites, some partially broken. **c** – Miners recovering the loose material after retrieving the stalactites. **d** – Other area of the cavity with the stalactites still *in situ.* Photographs courtesy of Eng. F. Álvarez. Scale bar: 20 cm.

replaced by laths of marcasite. Toward the edge of some stalactites, layers of "capillitite", the brown-colored variety of rhodochrosite, up to 1 mm thick, alternate with pink bands of rhodochrosite (Fig. 4a) and are commonly associated with irregular layers of pyrite ± marcasite.

In some cases, the cross-sections of the stalactites show crenulated layers of rhodochrosite crystals, darker in the central parts and paler towards the borders, with alternating layers of different intensities of pink color; we refer to these stalactites as maple leaf stalactites (Fig. 4b, c), owing to their resemblance to the leaves of those trees.

Another peculiar internal pattern of these stalactites, originally called by us "stalactite flowers", consists of six radial and zoned composite crystals, with a more-or-less central feeder, in some cases difficult to visualize (Fig. 4d, e). One or more of the individual petals may show the maple leaf pattern (Fig. 4d). Many years later, this habit was named by Behnke (2016) as a trapiche rhodochrosite or trapiche-like rhodochrosite "flowers".

The stalactites have a roundish termination (Fig. 2d) with smooth or undulated surfaces, which may be encrusted with small tabular crystals of baryte, whereas others develop a "poker chip-like" texture (Fig. 4f), which is also known in calcite.

On occasions, the stalactites are very small, 2 or 3 cm long and only a few millimeters in diameter and develop a conical shape, looking more like icicles than stalactites (Fig. 4g), but, in spite of that external shape, they have an internal channel, so they are true stalactites. There is evidence of a similar but larger arrangement, up to 8 cm in length (Fig. 4h), a rare example in which a segment of the upper part of two feeders was recovered *in situ*, along with the rest of the stalactites.

The color of the stalactite bands encompasses a wide range of hues from white to whitish-pink or very pale pink (Fig. 5a), in some cases with a yellowish hue, to deep raspberry pink (Fig. 5b) or combinations of these colors (Fig. 5c) and various shades of brown associated with pink bands (Fig. 5d).

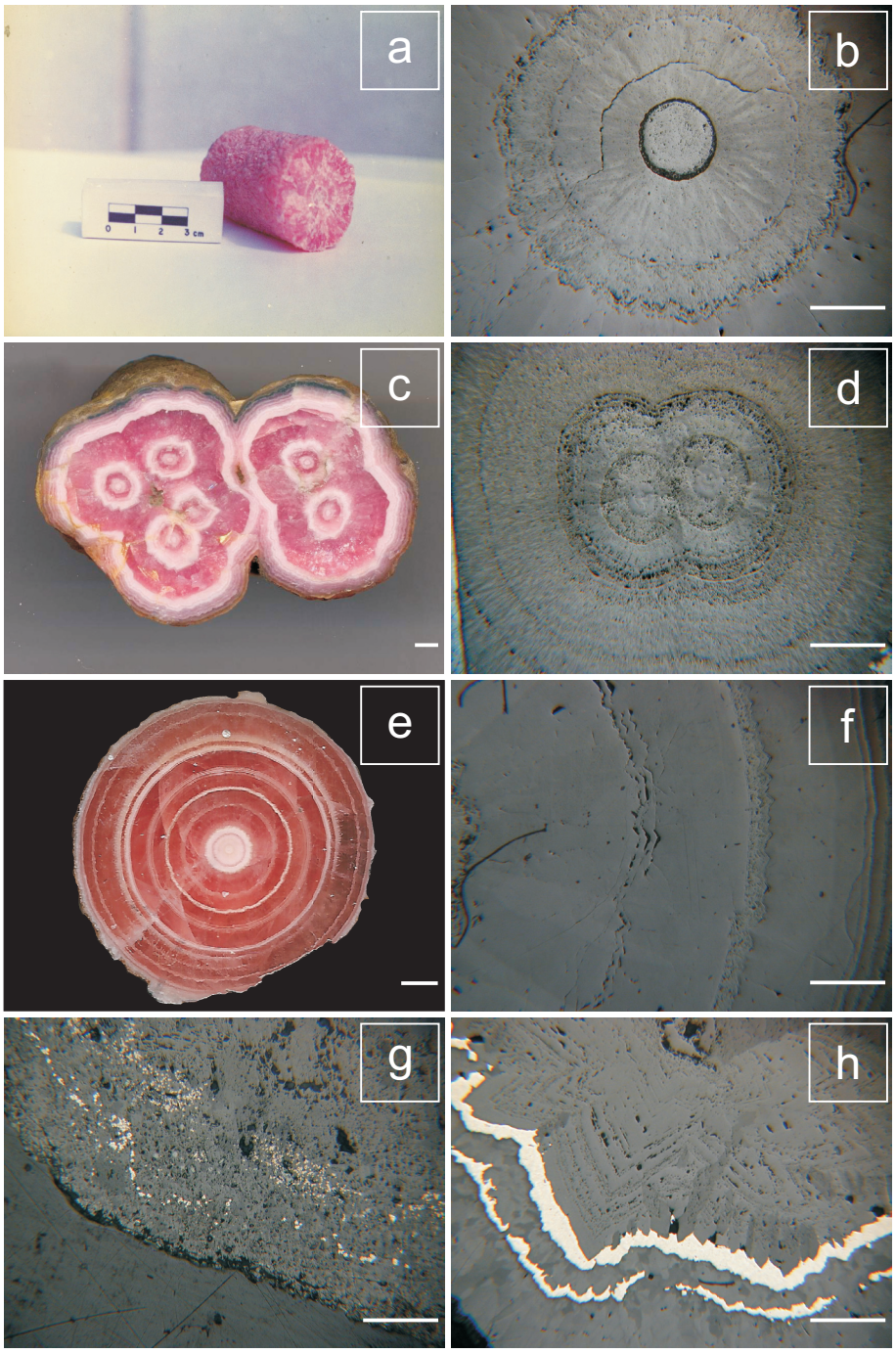

Fig. 3a – Photograph and **b** – photomicrograph of a single stalactite. **c** – Photograph and **d** – photomicrograph of stalactites with several independent feeders. **e** – Photograph where the different layers seems to be separated by clean boundaries. **f** – Photomicrograph showing the irregular and crenulated boundaries between layers. **g** – and **h** – Photomicrographs showing pyrite, arranged in bands, following the scalloping produced by the rhodochrosite crystals. Scale bar: 2 mm.

3.2. Helictites

Along with stalactites, helictites are also present. Helictites are curved twig-like cave deposits, usually of calcite, that grow at the free end by deposition from water emerging therefrom a nearly microscopic central canal (Bates and Jackson 1980). Helictites in Capillitas are smaller than stalactites, both in length and diameter and take on different shapes, living up to their name (Fig. 5e, f, g). However, according to the verbal communications with Eng. F. Álvarez and some other mine workers, no helictites were found outside the smaller cavity discovered in 1986, and while several samples were recovered hanging from the ceiling of the cavity, there is no photographic record of their *in situ* occurrence.

The helictites are generally less than a few mm in diameter and in some instances, reach 15 cm in length. All have an internal channel that varies in diameter from a few micrometers to 1 mm. Their colors are generally paler than the stalactites and range from light pink to white. In some cases, there is a layer of "capillitite" close to the outer rim that wraps around several individual helictites (Fig. 5h); in some cases, the layer of "capillitite" is covered by a thin black film of manganese oxides. Like stalactites, some of the helictites develop a "poker chip-like" texture, but with more delicate thickness.

3.3. Chemical Composition

Chemical analyses were performed along eight transects. In order to have a wider panorama of their chemical composition, five different sample types were selected: (1) one single stalactite with pale and raspberry pink alternating bands (Fig. 3e, sample 1254); (2) one composite helictite with several feeders, with alternating layers of different shades of light-pink color and an external band of "capillitite", partially associated with pyrite, that may wrap several helictites (Fig. 5h, sample 1260); this polished section is a fragment cut from a larger sample (Fig. 5g); (3) one

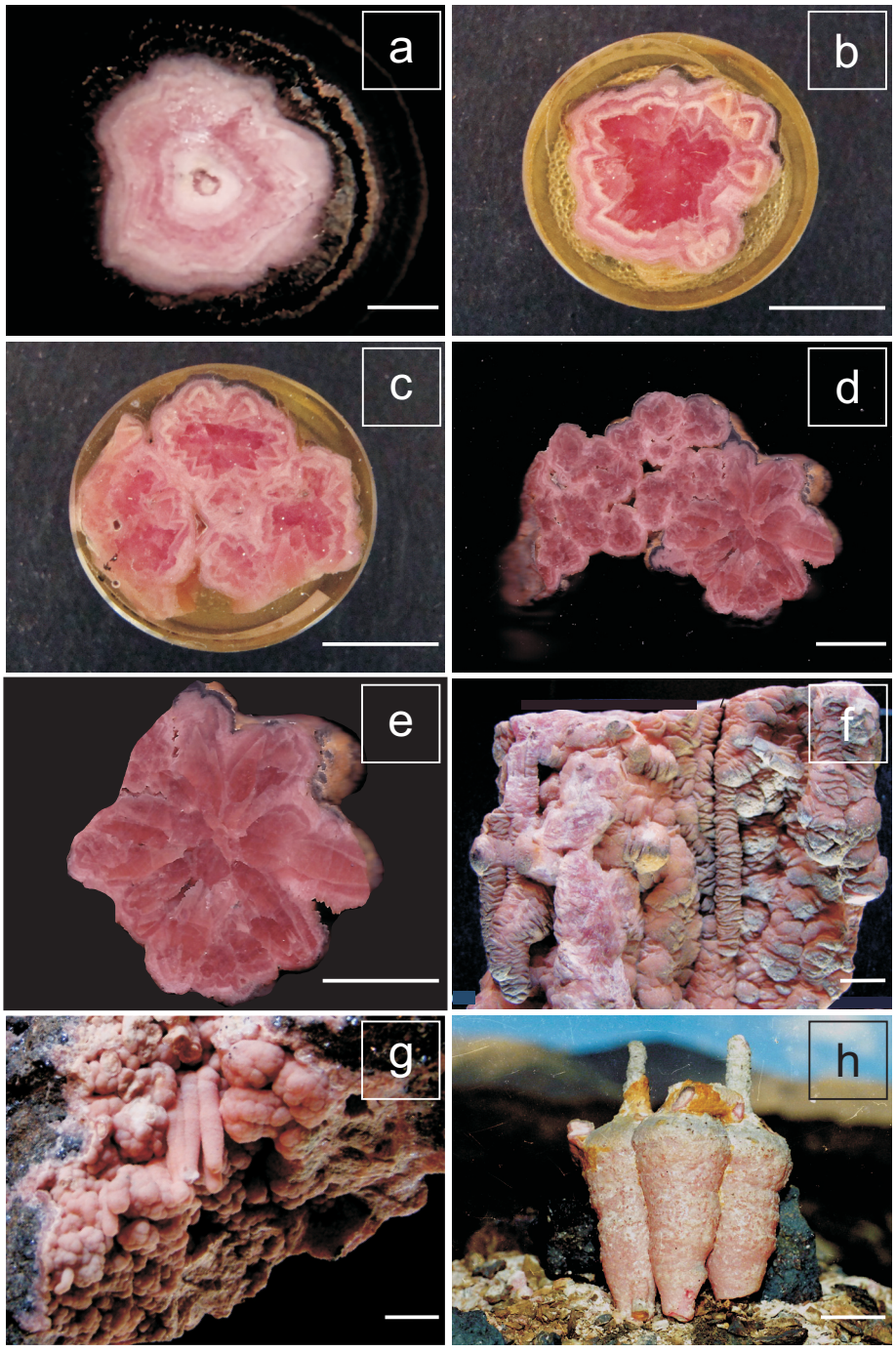

Fig. 4a –Thin layer of "capillitite" ± pyrite outlining a stalactite. **b** – and **c** – Stalactite with maple leaf texture. **d** – Stalactites with maple leaf and "flower"/trapiche-like textures. **e** – Detailed of 4d, enhancing the area with the "flower"/trapiche-like texture. **f** – Stalactites with poker chip-like texture. **g** – Icicle-like stalactites. **h** – Conic stalactites with a segment of the upper part of two feeders. Photograph 4h courtesy of Eng. F. Álvarez Scale bar: 1 cm.

composite stalactite with a maple leaf texture (Fig. 4c, sample 1261); (4) one composite stalactite with several independent feeders, and alternating layers of very pale pink colors (Fig. 5a, sample 1288) and (5) one banded, non-stalactitic rhodochrosite with pink and brown layers sampled from the ceiling of the largest cavity (sample 1272). Representative results are shown in Tab. 1, analyses 1260a-424, 1260b-124 and 550, 1272-193 and 245 correspond to "capillitite", whereas the rest appertain to the various shades of pink rhodochrosite.

The chemical composition of the stalactitic rhodochrosite is fairly variable among layers, although they show roughly similar chemical patterns among the different samples (Fig. 6). The chemical composition of the helictite sample (1260), which includes layers of "capillitite", reflects this overall similarity, although the patterns show greater similarities within the individual stalactite (1254) than with the other two stalactitic samples (1261 and 1288), which more resemble the results for banded, non-stalactitic rhodochrosite (1272).

Zoning is due to variations in CaO, MgO, FeO and ZnO concentrations at the expense of MnO. The MnO invariably predominates over the other oxides. As the variation diagrams show (Fig. 6), the decrease in MnO is associated with an increase in the other four main oxides, especially in CaO, MgO and FeO; in most samples ZnO is invariant. The sample 1260 is different because in this specimen, the brown variety of rhodochrosite is present and its composition is associated with higher values of FeO and ZnO. Fig. 6 shows that most of the diagrams have linear patterns with negative trends, whereas the rest of the data are grouped in clusters. The participation of the other oxides is minor, with less than 0.05 wt. % each on average, with exceptional values that go up to (in wt. %) 0.49 SO_2, 0.20 CoO, 0.13 CdO and BaO, and 0.08 SrO.

In order to evaluate the distribution of the five main oxides in the different transects of analyzes, and the possible correspondence among them and the various color bands of the stalactites, the photographs of the analyzed

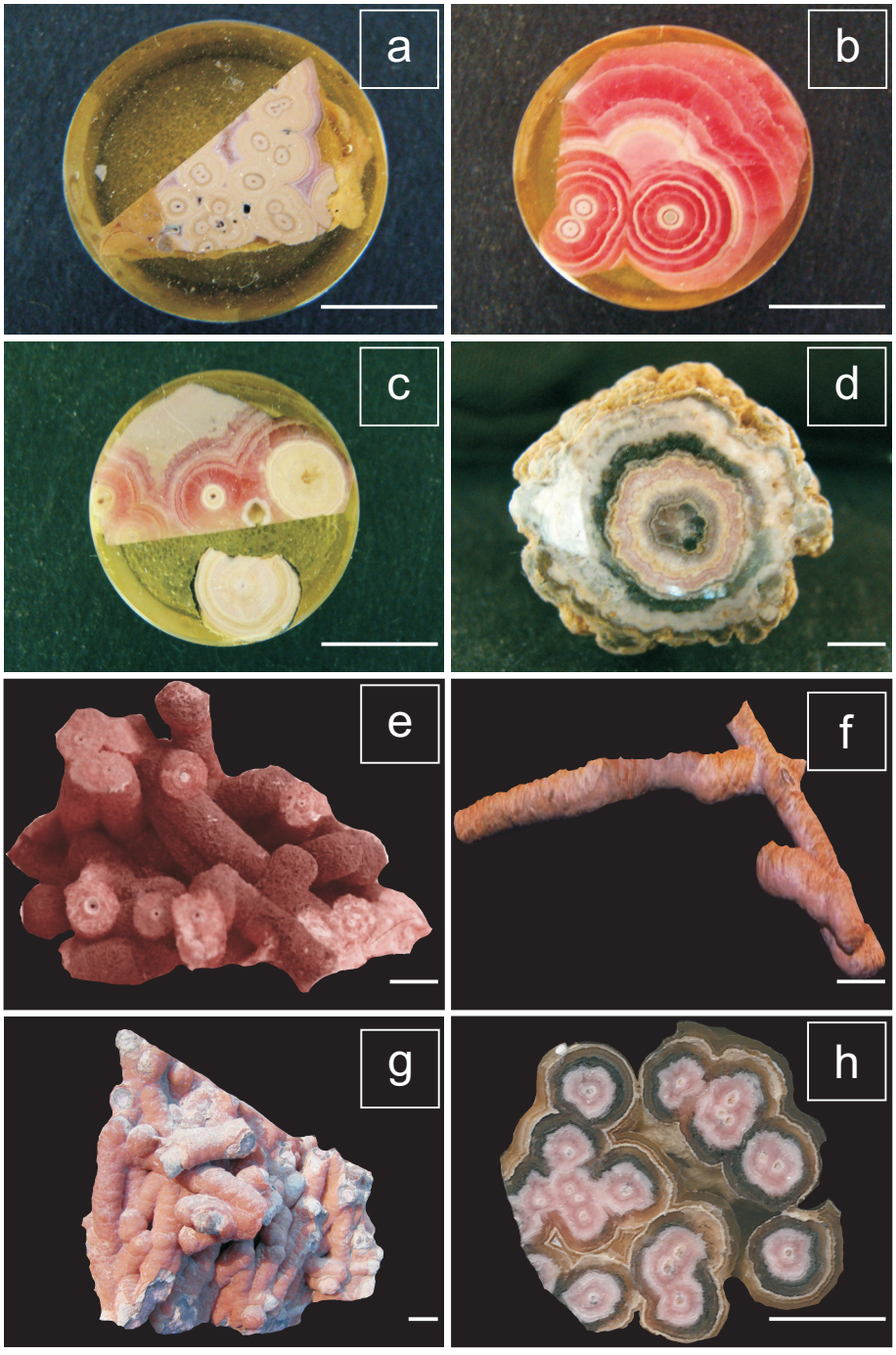

Fig. 5 Different colored stalactites. **a** – Very light pink stalactites. **b** –Stalactite of deep raspberry color, alternating with paler pink and white colored bands. **c** – Combinations of most of the previous colors. **d** – Several tints of brown ("capillitite"), alternating with pink and white colored bands. **e**, **f** , and **g** – Various presentations of helictites. **h** – Section of 5g showing "Capillitite" surrounding individual helictites and sometimes wrapping several into one group. Scale bar: 1 cm

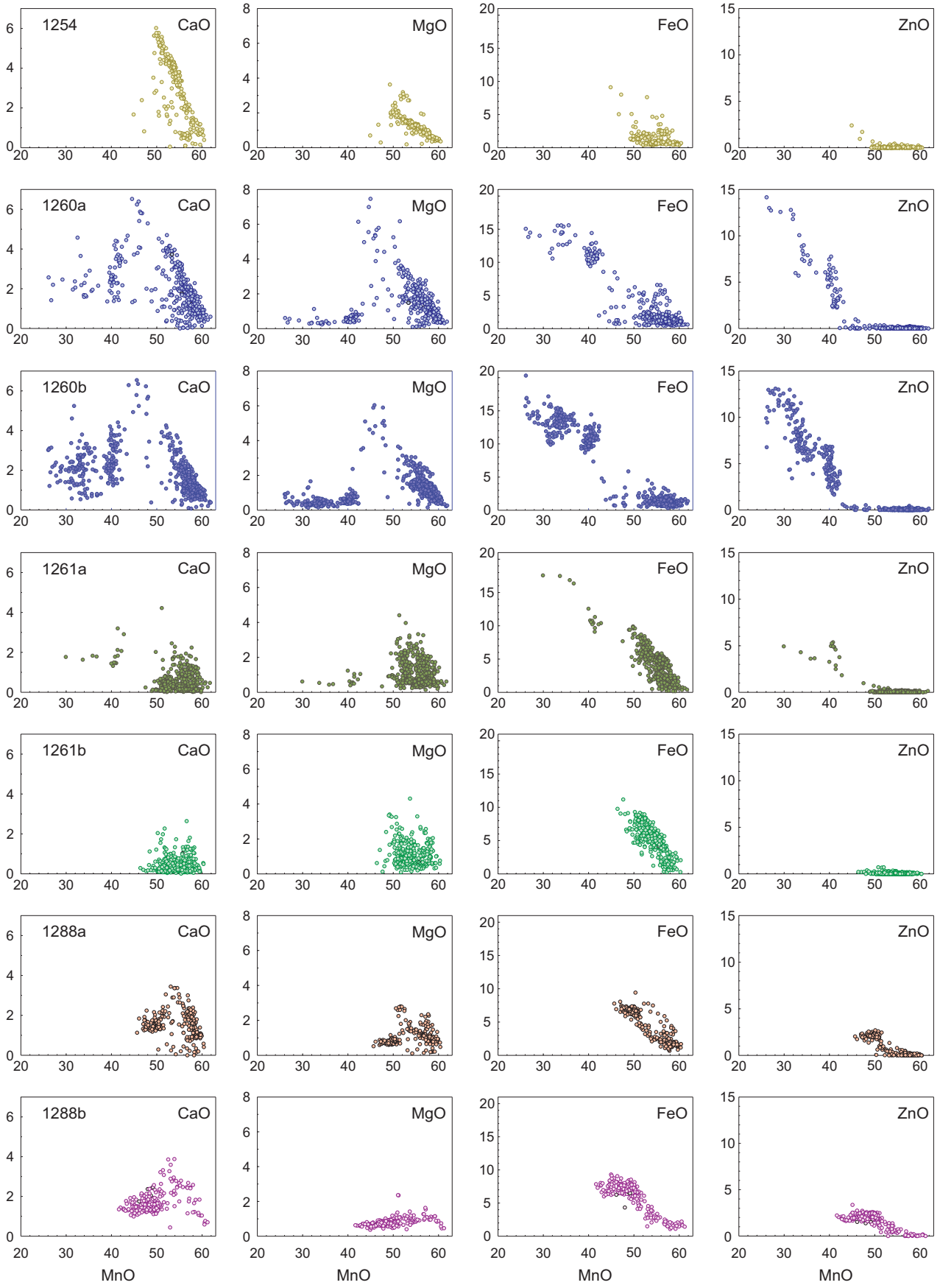
1254
1260a
1260b
1261a
1261b
1288a
1288b
CaO
MgO
FeO
ZnO
MnO

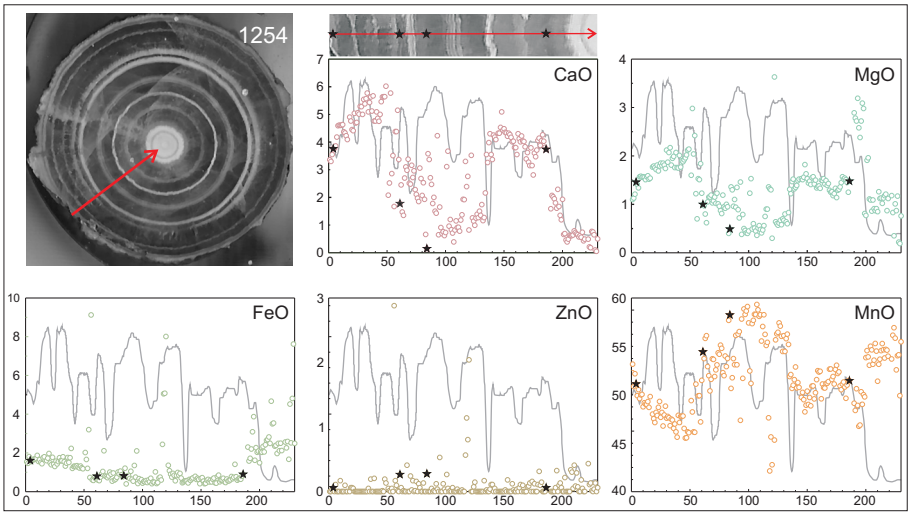

Fig. 7 Distribution of the five main oxides along the analyses transect carried out on sample 1254. Photograph of the sample converted to the grayscale and processed with the ImageJ software. The gray lines represent the different intensities of gray as in the image; it can be seen that there is no direct correlation between different intensities of gray and compositions. The black stars in all diagrams show the position of the analyses shown in Tab. 1.

samples were converted to the grayscale and processed with the ImageJ software (Fig. 7). What seems to work fairly well with back-scattered electron (BSE) images do not carry over with these photographs. It is clear that the increases of CaO and MgO accompany the decreases in the contents of MnO, whereas for FeO and ZnO the relationship is not so obvious owing to the limited contribution of these oxides.

The two trends of analyses performed on sample 1260 (Fig. 8) show better the relationships of FeO and ZnO with MnO and the other two oxides. Fig. 8b, especially, shows that in the areas where "capillitite" occurs, the concentrations of FeO and ZnO increase, whereas those of MnO decrease; the increment of these two oxides is generally accompanied by smaller drops in the CaO and MgO contents.

Both transects carried out on rhodochrosite sample 1261with the maple leaf texture (Fig. 9) show similar relationships among the main oxides. Here and in sample 1288 (Fig. 10), although there is no "capillitite", FeO and, to a lesser extent, ZnO are presently associated with the areas where the pink color is paler.

The analyses performed on the banded, non-stalactitic pink and brown rhodochrosite (sample 1272) yielded similar results (Fig. 11a) to those depicted in Fig. 6. This applies especially to those of the single-cylinder banded stalactite (sample 1254) of the same occurrence and to the helictites (sample 1260) of the smaller cavity. Figure 11b shows the distribution of the four main oxides plotted against MnO; the results show a possible miscibility gap between approximately 40 and 46 wt. % MnO, but this gap is not evident in Fig. 6, samples 1260a and b, where "capillitite" is also present. In order to further investigate this possible gap mentioned above, a plot of MnO + CaO versus the MgO + FeO + ZnO was made (Fig. 12).

⇦

Fig. 6 Variation diagrams of concentrations (wt. %) of MnO plotted against (from left to right) CaO, MgO, FeO and ZnO, separated into rows for each sample and transect of analyses.

3.4. X-ray powder diffraction

Twenty individual zones from seven representative stalactites, as well as four bands from banded rhodochrosite and one with a massive texture, were chosen for X-ray powder-diffraction scans. The bands of the brown variety are very thin and preclude their separation without contamination with the associated pink bands. We chose a representative sample of banded "capillitite" and selected samples from seven consecutive bands, sampled from the ceiling of the main cavity. Unit-cell parameters of the different zones of all samples are shown in Tab. 2 and plotted in Fig. 13.

4. Discussion

For the size and localized abundance, the stalactites of rhodochrosite described here are, as far as we know, the only occurrence of this type ever found. Kojima and Sugaki (1983) have studied a small sample (up to 12 cm long and 3 cm in diameter) of stalagmite-like rhodochrosite, also referred to as a bamboo shoot-shaped stone that grew at the bottom of a druse in the Oe mine, in Hokkaido, Japan. They did not mention stalactites in that deposit, and the true nature of a hydrothermal stalagmite was not demonstrated. Their results show chemical compositions and cell dimensions similar to those presented in this work (Tab. 3).

4.1. Conditions of formation of the stalactites

Since the Roman time of Plinius, stalactites have caught the attention of scientists. Many explanations, some based

Tab. 1 Representative chemical compositions of stalactitic, helictitic and banded rhodochrosite from 25 de Mayo vein (levels –12 and –8)

Sample	1254 (stalactite)				1260-a (helictite)				1260-b (helictite)				1261-a (stalactite)			
Analysis	4	61	84	186	327	376	411	424	59	88	124	550	25	275	362	521
MnO wt. %	53.90	56.55	59.60	54.17	53.32	52.78	52.93	40.02	53.53	52.47	41.62	42.26	57.21	54.94	57.68	51.10
FeO	1.61	0.80	0.82	0.90	1.34	0.49	1.82	12.05	0.84	1.29	11.05	12.51	0.22	5.66	0.24	4.41
ZnO	0.05	0.22	0.23	0.05	0.00	0.00	0.05	6.37	0.00	0.00	2.29	4.16	0.10	0.00	0.10	0.04
CaO	3.76	1.78	0.15	3.74	2.96	4.16	4.15	1.79	3.24	3.64	4.20	1.57	1.83	0.13	2.24	4.22
MgO	1.46	1.00	0.49	1.48	2.64	3.08	1.73	0.41	2.58	2.67	0.99	0.38	1.27	0.35	1.43	0.56
SO_2	0.03	0.09	0.03	0.00	0.04	0.05	0.00	0.00	0.03	0.00	0.08	0.04	0.00	0.05	0.00	0.03
CoO	0.00	0.00	0.06	0.00	0.03	0.00	0.00	0.00	0.00	0.00	0.00	0.05	0.04	0.00	0.00	0.00
SrO	0.00	0.00	0.00	0.03	0.00	0.00	0.00	0.00	0.00	0.00	0.00	0.06	0.00	0.03	0.00	0.00
CdO	0.00	0.00	0.00	0.00	0.00	0.00	0.00	0.00	0.00	0.00	0.00	0.00	0.00	0.00	0.00	0.00
BaO	0.00	0.00	0.00	0.00	0.00	0.00	0.00	0.00	0.00	0.00	0.00	0.00	0.00	0.00	0.00	0.00
CO_2	39.04	38.31	38.33	38.75	39.18	39.74	39.13	37.51	39.13	39.11	38.32	37.89	38.53	38.12	39.31	38.39
Total	99.85	98.75	99.71	99.12	99.51	100.30	99.81	98.15	99.35	99.18	98.55	98.92	99.20	99.28	101.00	98.75
Mn^{2+} *apfu*	1.713	1.832	1.929	1.735	1.689	1.648	1.679	1.324	1.698	1.664	1.348	1.384	1.842	1.788	1.821	1.652
Fe^{2+}	0.051	0.026	0.026	0.028	0.042	0.015	0.057	0.394	0.026	0.040	0.353	0.405	0.007	0.182	0.007	0.141
Zn^{2+}	0.001	0.006	0.006	0.001	0.000	0.000	0.001	0.184	0.000	0.000	0.065	0.119	0.003	0.000	0.003	0.001
Ca^{2+}	0.151	0.073	0.006	0.151	0.119	0.164	0.166	0.075	0.130	0.146	0.172	0.065	0.075	0.005	0.089	0.173
Mg^{2+}	0.082	0.057	0.028	0.083	0.147	0.169	0.097	0.024	0.144	0.149	0.056	0.022	0.072	0.020	0.079	0.032
S^{4+}	0.001	0.003	0.001	0.000	0.001	0.002	0.000	0.000	0.001	0.000	0.003	0.001	0.000	0.002	0.000	0.001
Co^{2+}	0.000	0.000	0.002	0.000	0.001	0.000	0.000	0.000	0.000	0.000	0.000	0.002	0.001	0.000	0.000	0.000
Sr^{2+}	0.000	0.000	0.000	0.001	0.000	0.000	0.000	0.000	0.000	0.000	0.000	0.001	0.000	0.001	0.000	0.000
Cd^{2+}	0.000	0.000	0.000	0.000	0.000	0.000	0.000	0.000	0.000	0.000	0.000	0.000	0.000	0.000	0.000	0.000
Ba^{2+}	0.000	0.000	0.000	0.000	0.000	0.000	0.000	0.000	0.000	0.000	0.000	0.000	0.000	0.000	0.000	0.000
C^{4+}	2.000	2.000	2.000	2.000	2.000	2.000	2.000	2.000	2.000	2.000	2.000	2.000	2.000	2.000	2.000	2.000
CATSUM	3.999	3.997	3.999	4.000	3.999	3.998	4.000	4.000	3.999	4.000	3.997	3.999	4.000	3.998	4.000	3.999

Sample	1261-b (stalactite)				1288-a (stalactite)				1288-b (stalactite)				1272 (banded texture)			
Analysis	7	36	53	112	74	79	248	258	14	18	97	265	193	245	351	408
MnO wt. %	58.28	55.88	52.36	57.92	53.95	56.91	53.15	50.33	49.85	52.36	53.74	52.78	34.02	34.16	56.03	58.49
FeO	0.73	2.19	6.49	2.27	2.10	1.62	7.78	9.42	7.20	5.28	3.13	3.30	13.75	10.73	2.34	0.11
ZnO	0.00	0.00	0.03	0.00	0.00	0.00	0.00	0.05	1.98	1.28	0.37	0.68	8.46	15.81	0.00	0.00
CaO	1.32	1.21	0.96	0.26	3.37	1.82	0.24	0.29	1.51	1.66	2.95	3.27	3.84	0.84	1.40	1.58
MgO	0.91	1.32	0.87	0.88	1.55	1.21	0.29	0.93	0.66	1.01	1.09	1.00	0.82	0.13	1.18	0.80
SO_2	0.00	0.05	0.00	0.00	0.09	0.00	0.04	0.00	0.00	0.00	0.05	0.00	0.10	0.00	0.00	0.00
CoO	0.00	0.00	0.00	0.00	0.05	0.00	0.06	0.08	0.00	0.00	0.00	0.00	0.00	0.13	0.00	0.00
SrO	0.00	0.00	0.05	0.03	0.00	0.04	0.00	0.00	0.00	0.00	0.00	0.00	0.00	0.00	0.00	0.00
CdO	0.05	0.00	0.00	0.00	0.03	0.00	0.13	0.00	0.03	0.00	0.00	0.04	0.00	0.00	0.00	0.07
BaO	0.00	0.00	0.00	0.00	0.00	0.00	0.00	0.00	0.00	0.00	0.00	0.00	0.00	0.09	0.00	0.00
CO_2*	38.65	38.47	38.20	38.50	39.26	39.07	38.38	38.31	38.32	38.82	39.03	38.81	38.15	37.22	38.58	38.49
Total	99.94	99.12	98.96	99.86	100.40	100.67	100.07	99.41	99.55	100.41	100.36	99.88	99.14	99.11	99.53	99.54
Mn^{2+} *apfu*	1.871	1.802	1.701	1.867	1.705	1.808	1.718	1.630	1.614	1.674	1.708	1.688	1.106	1.139	1.802	1.885
Fe^{2+}	0.023	0.070	0.208	0.072	0.066	0.051	0.248	0.301	0.230	0.167	0.098	0.104	0.442	0.353	0.074	0.004
Zn^{2+}	0.000	0.000	0.001	0.000	0.000	0.000	0.000	0.001	0.056	0.036	0.010	0.019	0.240	0.459	0.000	0.000
Ca^{2+}	0.054	0.049	0.039	0.011	0.135	0.073	0.010	0.012	0.062	0.067	0.119	0.132	0.158	0.035	0.057	0.064
Mg^{2+}	0.051	0.075	0.050	0.050	0.086	0.068	0.017	0.053	0.038	0.057	0.061	0.056	0.047	0.008	0.067	0.045
S^{4+}	0.000	0.002	0.000	0.000	0.003	0.000	0.001	0.000	0.000	0.000	0.002	0.000	0.004	0.000	0.000	0.000
Co^{2+}	0.000	0.000	0.000	0.000	0.001	0.000	0.002	0.002	0.000	0.000	0.000	0.000	0.000	0.004	0.000	0.000
Sr^{2+}	0.000	0.000	0.001	0.001	0.000	0.001	0.000	0.000	0.000	0.000	0.000	0.000	0.000	0.000	0.000	0.000
Cd^{2+}	0.001	0.000	0.000	0.000	0.001	0.000	0.002	0.000	0.001	0.000	0.000	0.001	0.000	0.000	0.000	0.001
Ba^{2+}	0.000	0.000	0.000	0.000	0.000	0.000	0.000	0.000	0.000	0.000	0.000	0.000	0.000	0.000	0.000	0.000
C^{4+}	2.000	2.000	2.000	2.000	2.000	2.000	2.000	2.000	2.000	2.000	2.000	2.000	2.000	2.000	2.000	2.000
CATSUM	4.000	3.998	4.000	4.000	3.997	4.000	3.999	4.000	4.000	4.000	3.998	4.000	3.996	4.000	4.000	3.999

* Determined by stoichiometry. Formula contents on the basis of 6 *apfu*. CATSUM – the sum of cations.

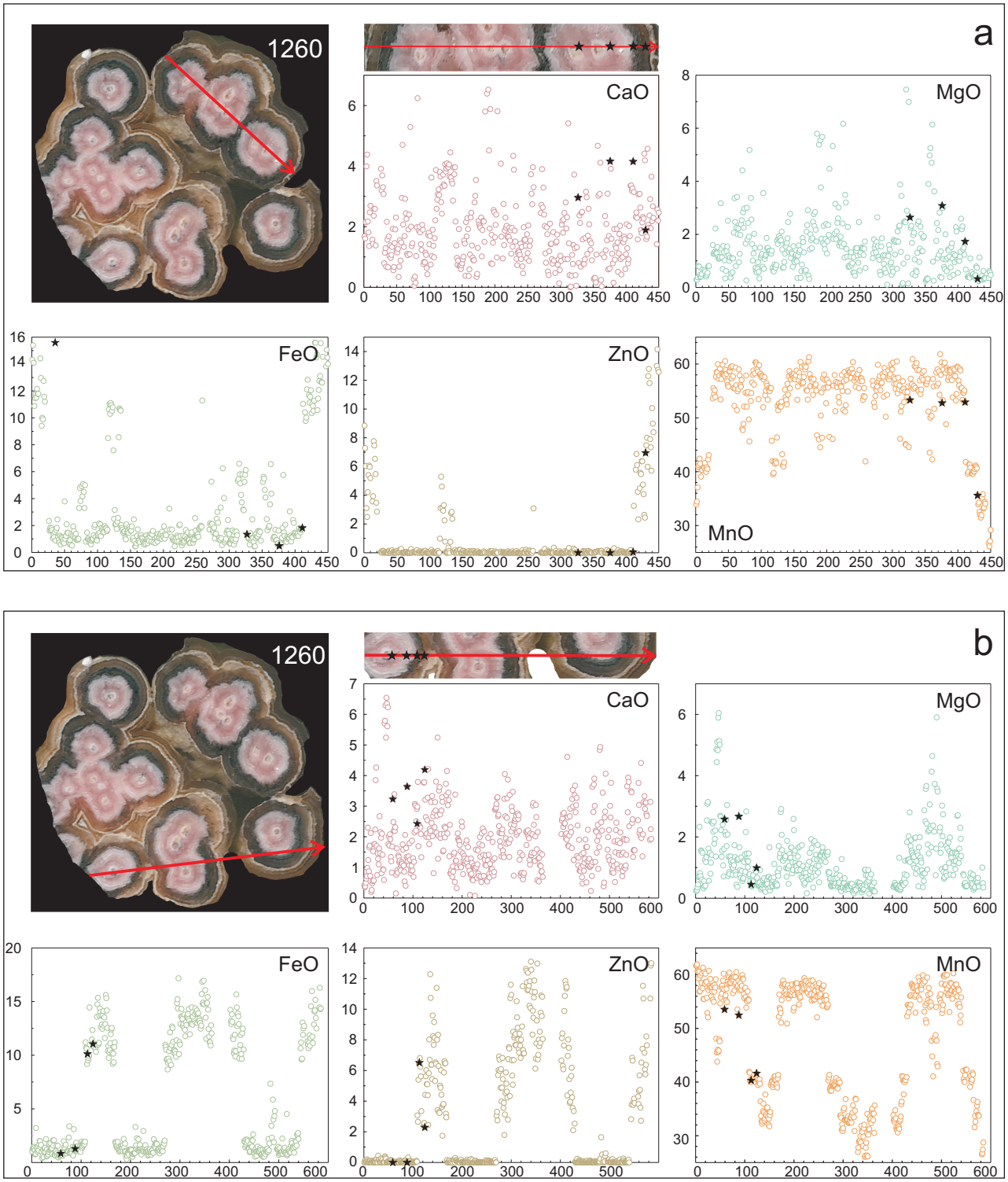

Fig. 8 a and **b** – The two trends of analyses performed on sample 1260 with the distribution of the main oxides along the analysis line. The black stars in all diagrams show the position of the analyses shown in Tab. 1.

on observation and others on religious beliefs, have been proposed to explain their origin.

Many factors converge in the formation of stalactites. Some of them include an appropriate setting, a flow of significantly saturated fluids, and a proper evaporation rate. Although most of what is reported on the subject was done on supergene stalactites grown in karstic environments, some of the basic principles apply to the epithermal stalactites of rhodochrosite studied here. As many authors agree (e.g., Goto 1958; Moore 1962; Shaub 1972;

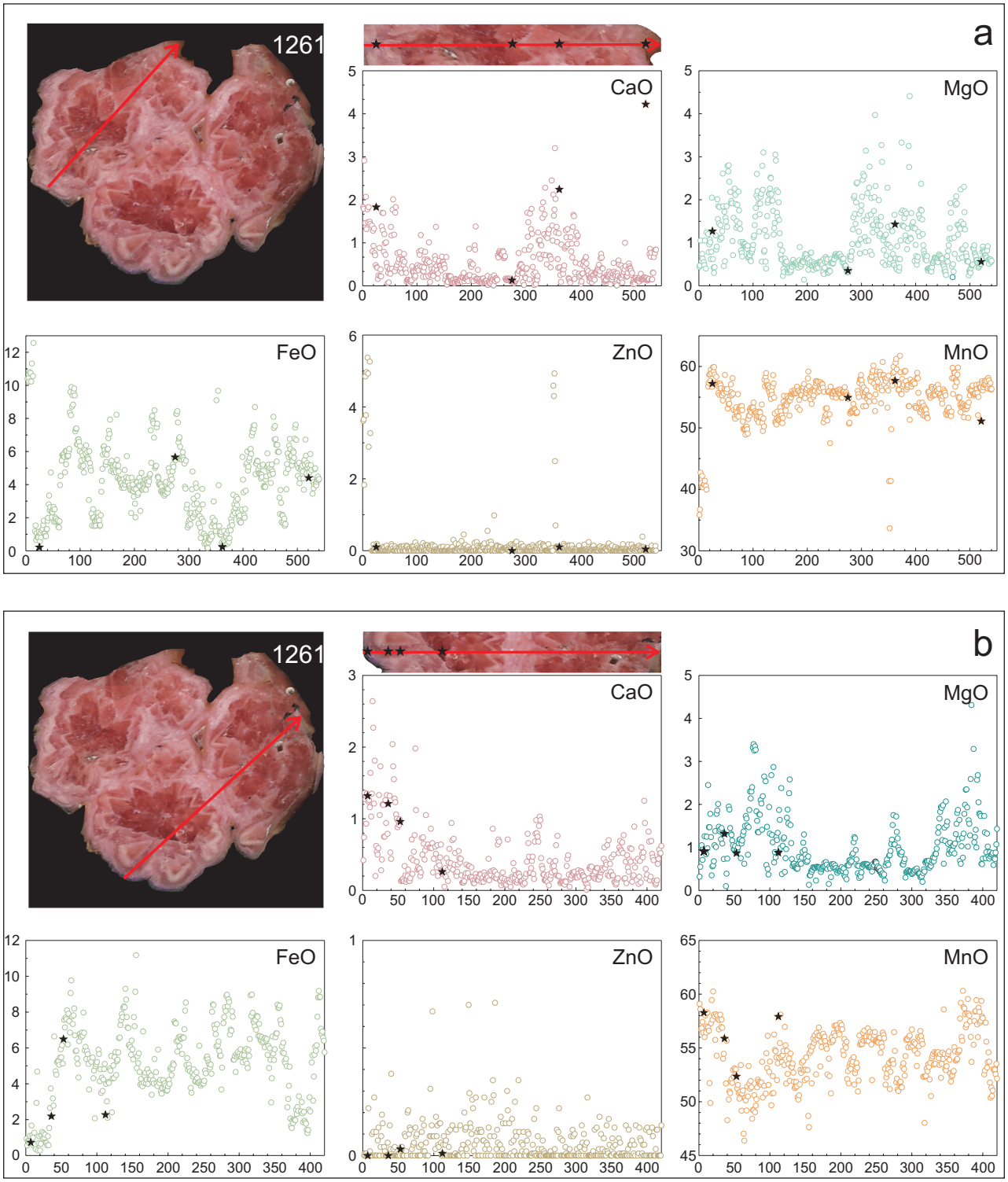

Fig. 9 a and **b** – The two trends of analyses performed on sample 1261 with the distribution of the main oxides along the analyses line. The black stars in all diagrams show the position of the analyses shown in Tab. 1.

Maltsev 1998; Frisia 2019), the growth of stalactites is complex and can be summarized as the combination of two main processes. The stalactites grow longitudinally due to the infiltration of oversaturated bicarbonate solutions. While dripping, each drop loses part of the CO_2, leading to the precipitation of carbonates around it; the repetition of this process will create a central channel along which the solutions travel. In the meantime, the solutions will flow on the outside of the stalactite, depositing a crust. When several stalactites grow close to

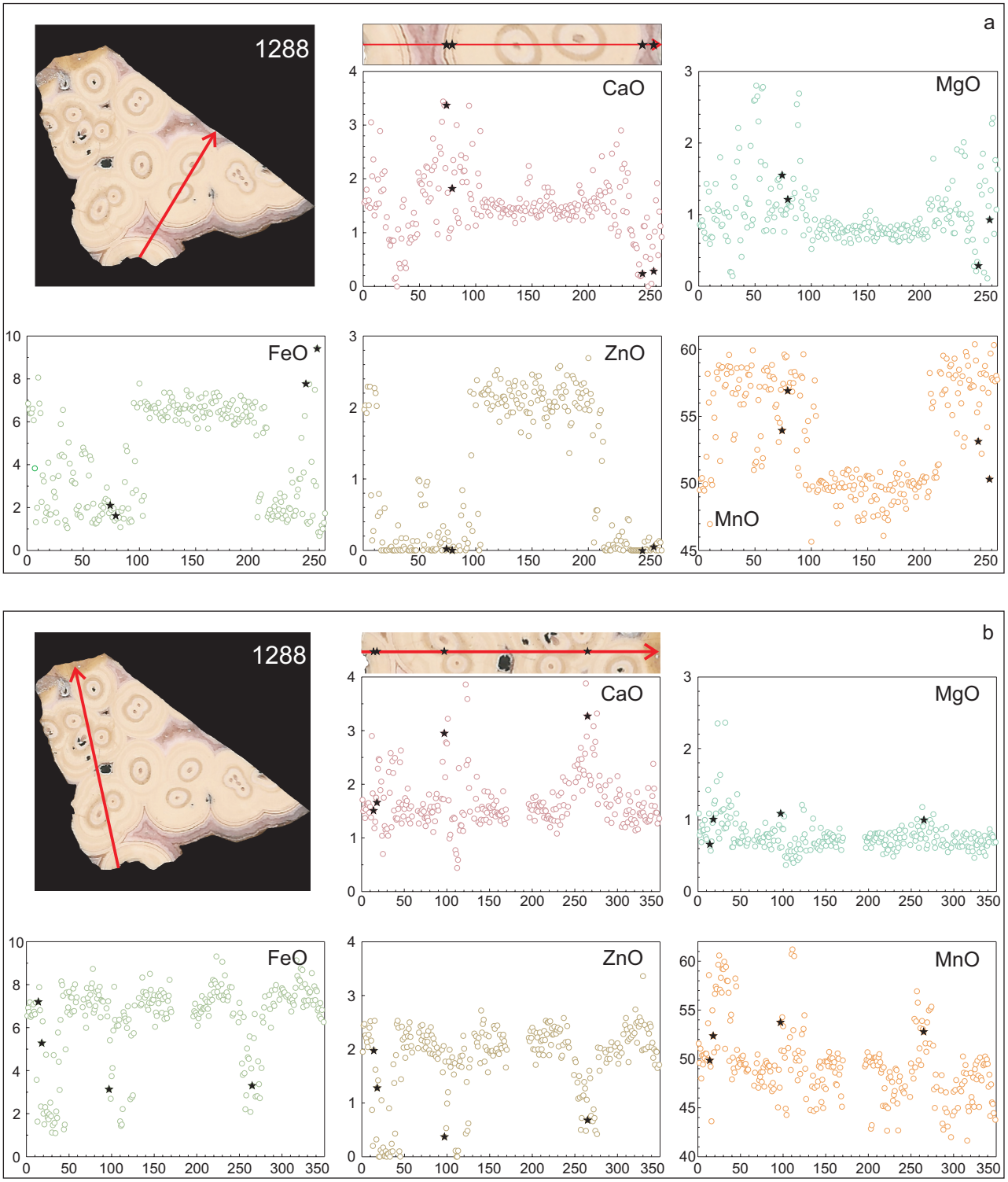

Fig. 10 a and **b** – The two trends of analyses performed on sample 1288 with the distribution of the main oxides along the analysis line. The black stars in all diagrams show the position of the analyses shown in Tab. 1.

one another, the solutions flowing along the outer part, at one point, will enclose several of them, grouping them together to form what on the outside looks like a single stalactite. A cross-section, shows the individual stalactites with their respective feeders (Figs 3c, d, and 5a, b, c). The stalactites shown in Fig. 4h, which were recovered *in situ* from the ceiling of the smaller cavity, may represent a rare example where a segment of the feeder was recovered due to the softness of the material in this area of the cavity.

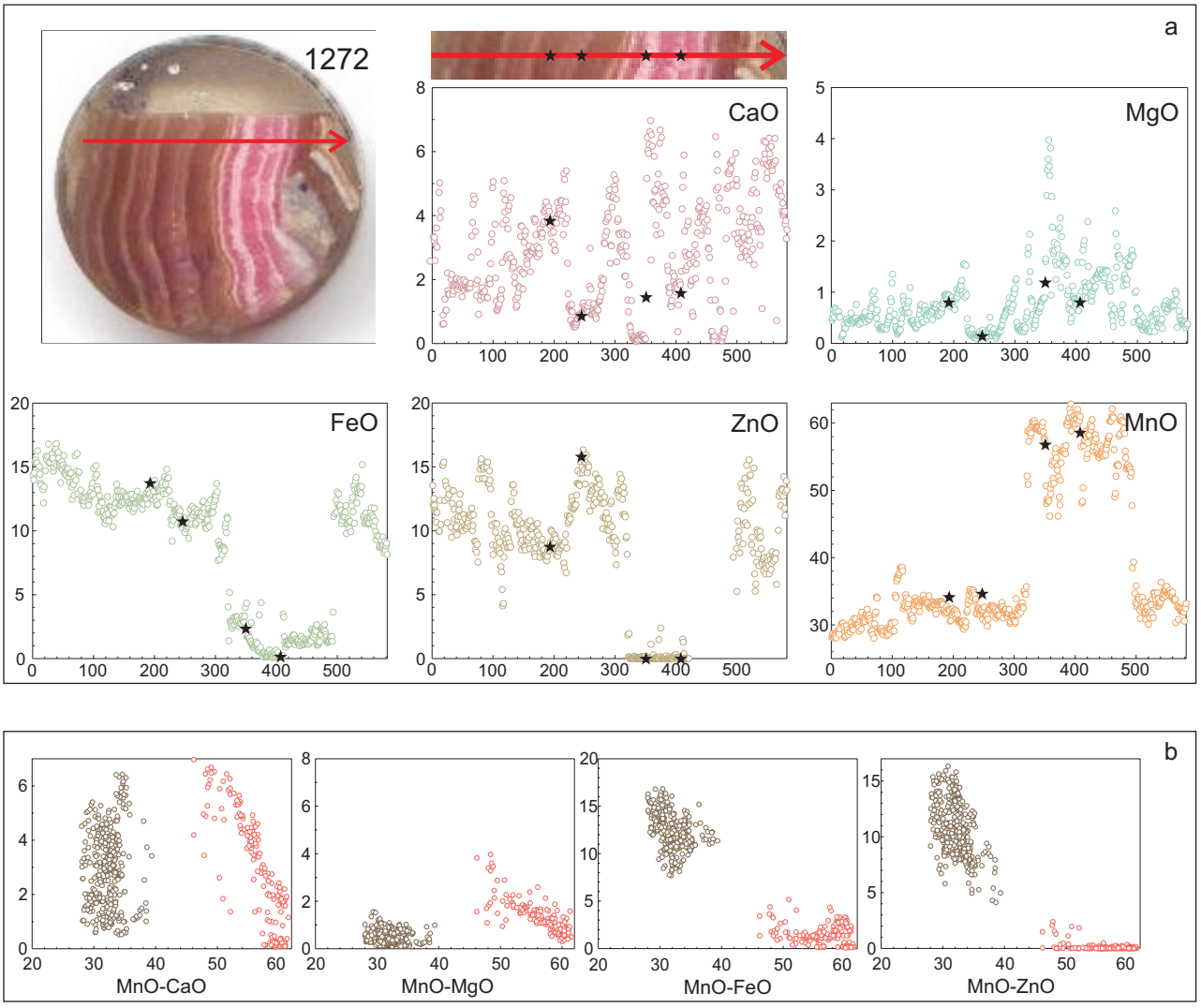

Fig. 11 a – The trend of analyses performed on sample 1272 with the distribution of the main oxides along the analysis line. The black stars in all diagrams show the position of the analyses shown in Tab. 1. **b** – Variation diagrams of concentrations (wt. %) of MnO plotted against (from left to right) CaO, MgO, FeO and ZnO. The black stars in all diagrams show the position of the analyses shown in Tab. 1.

The maple leaf and flower (trapiche-like) textures could be due to a temporary and partially sealed feeder so that fluids, which cannot pass through that seal, flow through the open spaces across the stalactite and develop perpendicularly, and in a more-or-less radial distribution, larger crystals of rhodochrosite.

Stalactites have previously been found in epithermal deposits as part of the hypogene mineralization (e.g., Barton and Campbell 1994; Cunningham et al. 1994; Campbell and Barton 1996, and references therein), but they correspond to sulfide or silica stalactites.

According to Campbell and Barton (1996), the presence of stalactites in epithermal deposits would indicate that portions of these systems that were below the paleo-water table had undergone, at least sporadically, localized blockages. This led to the presence of isolated sectors where the trapped boiling fluids produced a vapor phase that filled most of the pockets. In addition to the percolation of solutions from other conduits with free circulating fluids on the ceiling of the cavities, these conditions would generate an appropriate environment for the formation of stalactites. The remaining fluids on the bottom would be the reason for the scarcity or absence of stalagmites, as in this instance, and also in other epithermal deposits (Barton and Campbell 1994). In other words, the formation of these stalactites of rhodochrosite would require isolated gas cavities in a liquid-dominated hydrothermal system, somewhat like a large bubble in an inverted siphon, with liquid also saturating the pore space of the rocks at the top, and with hydrostatic conditions under some tens of meters of liquid water.

In view of the chemical compositions (Tab. 1, Figs 6, 11b, 12) and the unit cell dimensions (Tab. 2, Fig. 13) of both stalactitic and non-stalactitic rhodochrosite, the

same mineralizing fluids seem to be involved. Stalactites formed toward the end of the last stage of the mineralization, just after the banded rhodochrosite was deposited. Figures 7 to 10 show that the four main oxides that replace MnO are somewhat depleted compared to the results plotted in Fig. 11a; only MgO is a bit enriched in sample 1260; nonetheless, the general patterns (Figs 6 to 11) are all similar.

Fluid inclusion data, obtained on banded rhodochrosite from the 25 de Mayo vein, gave homogenization temperatures of 145 to 150 °C and salinities up to 4 wt. % NaCl(eq) (Márquez-Zavalía 1988), values that are within the expected range for this environment (e.g., Barton and Campbell 1994). Even though the vapor-dominant conditions under which the stalactites may have been formed, there is no direct evidence of a high concentration of CO_2 in the fluid inclusions. This fact was also observed in other deposits, as in Creede, Colorado, USA (Campbell and Barton 1996).

4.2. Color zoning as a result of chemical variations

The stalactites of rhodochrosite show zonation, which is a reflection of the variations in their chemical compositions as MnO is replaced, in different proportions, by the other four main oxides: CaO, MgO, FeO and ZnO (Tab. 1, Figs 6 to 11).

Where MnO predominates and is accompanied by small amounts of CaO, the pink color is more intense. Conversely, the paler shades are associated with areas poorer in MnO and richer in FeO accompanied by CaO and MgO and very little or no ZnO.

In the brown bands corresponding to "capillitite", FeO and ZnO (up to 20 and 15 wt. %, respectively) and, to a lesser extent, CaO replace MnO; note that MnO remains the predominant oxide.

When the composition of the stalactites is compared with that of the banded rhodochrosite sampled from the cavity ceiling, similar patterns are observed (Tab. 1, Fig. 11). In the brown areas, the depletion in MnO is associated with enrichment in FeO and ZnO. On the other hand, FeO and ZnO have little participation in the pink areas, whereas MnO predominates, associated with small proportions of CaO±MgO; nevertheless, the participation of those oxides increases in the palest pink bands with a yellowish tint.

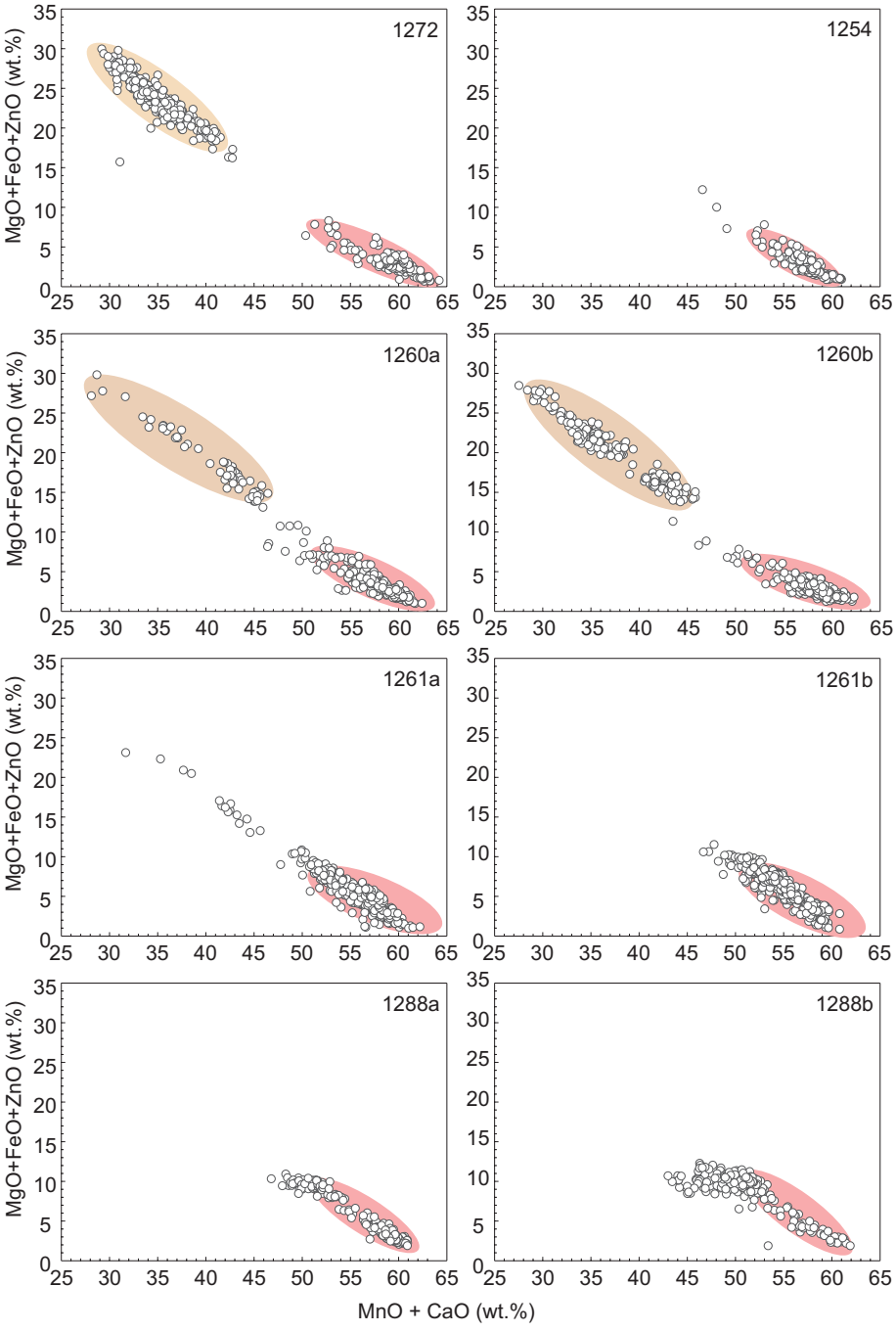

Fig. 12 Variation diagrams of concentrations (wt. %) of MnO+CaO plotted against MgO+FeO+ZnO for each of the analyzed samples.

Tab. 2 Unit-cell dimensions of rhodochrosite from Capillitas, Argentina

Sample	#	Texture	Description	Color	*a* (Å)	*c* (Å)	*V* (Å^3)
01	a	Two attached stalactites of rhodochrosite: (a) smaller, (b) bigger	Whole stalactite	Pinkish white	4.778(1)	15.691(1)	310.2
	b_1		External zone	Light pink	4.776(1)	15.668(1)	309.5
	b_2		Intermediate zone	Light pink	4.777(3)	15.658(2)	309.5
	b_3		Center	Pinkish white	4.775(1)	15.642(1)	308.9
04	a	Stalactitic rhodochrosite	External zone	Light pink	4.787(1)	15.705(1)	311.7
	b		Intermediate zone	Pink	4.771(1)	15.710(1)	309.7
	c		Center	Pink	4.770(3)	15.636(1)	308.1
15	a	Stalactitic rhodochrosite	External zone	Pink	4.775(1)	15.657(1)	309.2
	b		Second zone	Pink	4.774(1)	15.662(1)	309.2
	c		Third zone	Pink	4.777(1)	15.660(1)	309.5
	d		Fourth zone	Pinkish white	4.790(2)	15.799(1)	314.0
	e		Fifth zone	Light pink	4.781(1)	15.688(1)	310.5
	f		Sixth zone	Pinkish white	4.790(1)	15.777(1)	313.5
	g		Center	Pink	4.774(1)	15.642(1)	308.8
17	a	Stalactitic rhodochrosite	External zone	Light pink	4.788(1)	15.824(1)	314.2
	b		Second zone	Pink	4.783(1)	15.664(1)	310.4
18	a	Stalactitic rhodochrosite	External zone	Pinkish white	4.788(2)	15.605(1)	309.9
	b		Second+third zone	Pink	4.774(1)	15.793(1)	311.7
19	a	Stalactitic rhodochrosite	External zone	Pink	4.772(1)	15.648(1)	308.6
	b		Central zone, white	White	4.781(1)	15.810(1)	313.0
03	a	Banded rhodochrosite	External zone	Pink	4.778(1)	15.695(1)	310.3
	c		Third zone	Pink	4.781(2)	15.614(2)	309.1
	d		Fourth zone	Pink	4.777(2)	15.689(2)	310.1
05	-	Massive rhodochrosite		Pink	4.765(1)	15.627(1)	307.3
11	a	Banded "capillitite"	External zone	Medium brown	4.742(1)	15.636(1)	304.5
	b		Second zone	Light brown	4.739(1)	15.531(1)	302.1
	c		Third zone	Light brown	4.736(1)	15.461(1)	300.3
	d		Fourth zone	Medium brown	4.748(1)	15.574(1)	304.0
	e		Fifth zone	Light brown	4.736(1)	15.562(1)	302.3
	f		Sixth zone	Light brown	4.726(1)	15.501(1)	299.8
	g		Seventh zone	Med. brown	4.747(2)	15.642(1)	305.2

The substitution of MnO + CaO by the other oxides (MgO + FeO + ZnO) is shown in Fig. 12. There, compositions with more than 51 wt. % of MnO + CaO correspond to the darker shades of pink rhodochrosite (pink oval), whereas "capillitite compositions are located within the light brown oval, in the approximate range between 28 and 45 wt. % MnO + CaO; the rest of the plots correspond to the palest shades of pink rhodochrosite. The gap observed in sample 1272 is not replicated in the other samples, showing that it does not reciprocate to a gap in the rhodochrosite composition but instead appears to be sporadic for the composition of that particular sample.

4.3. Cell dimensions of the different colored bands of rhodochrosite

From the data obtained in this study (Tab. 2) there is not a consistent equivalence between the variations of the pink colors of rhodochrosite and the dimensions of the unit cell parameters. Nevertheless, most stalactites show a slight tendency to smaller values in the cell dimensions

Tab. 3 Unit-cell dimensions of rhodochrosite from different occurrences

Mineral	*a* (Å)	*c* (Å)	*V* (Å^3)	Reference
Rhodochrosite	4.7768	15.664		Goldschmidt and Graf (1957)
	4.777	15.67		Swanson et al. (1957)
	4.7771	15.664		Graf (1961)
	4.7682	15.6354	307.86	Effenberger et al. (1981)
Stalagmitic rhodochrosite	4.7729	15.6947		Kojima and Sugaki (1983)
	4.7804	15.7947		Kojima and Sugaki (1983)
Stalactitic rhodochrosite (avg., *n* = 24)	4.778(7)	15.690(6)	310.3(1.9)	This paper
"capillitite" (avg., *n* = 7)	4.739(7)	15.558(62)	302.6(1.9)	This paper

associated with the most intense pink colors; as the colors become paler, the values increase progressively (Fig. 13).

The difference that is most noticeable involves "capillitite", in which all the parameters are unquestionably smaller than those of pink rhodochrosite from Capillitas and other localities (Tab. 3). Among them, the paler colors are associated with smaller cell parameters (Fig. 13).

4.4. Helictites

Since helictites were first named and described (Dolley 1886; Moore 1954), various hypothesis have been developed about the origin of these exotic speleothems. Moore (1962) pointed out that helictites generally grow in small niches, filled with air at rest. Many authors (e.g., Huff 1940; Moore 1954; Andrieux 1965; Frisia et al. 2002; Onuk et al. 2014) agreed that fluid circulation through helictites is stimulated by hydrostatic pressure and capillary forces and that helictites form where the evaporation rate is higher than the flow rate. Some authors (e.g., Onuk et al. 2014) propose that another important factor is the presence of impurities that partially obstruct the internal channel. All authors agree that a true helictite, even though curved or even contorted, has an internal channel.

The epithermal helictites of rhodochrosite from Capillitas, were only found hanging from the ceiling of the smallest cavity, discovered in 1986, agreeing with the postulate of Moore (1954) that they mostly occur in small alcoves or cavities. All helictites found in Capillitas have an internal channel, are representative examples of helictites classified as "vermiform", and occur as dense groups in which the helictites are intertwined or crossed by others (Fig. 5f, g) or almost isolated (Fig. 5h). The fact that we did not observe or sample them *in situ*, that there are no photographic records of them inside the cavities and that currently, access to the caves is not possible prevents further interpretations, although their presence is worth mentioning.

5. Conclusions

For their size and localized abundance, the epithermal stalactites of rhodochrosite found in Capillitas are perhaps not unique in the world, but they are the only ones of that kind recorded in the literature.

In the 1985–86 finds, more than 20 tons of stalactites and a few small stalagmites were recovered; the presence of columns was never mentioned. There is no record of the amount recovered in the previous finds. Several helictites were also found hanging from the ceiling in the smallest cavity, along with pieces of broken stalactites on the ground.

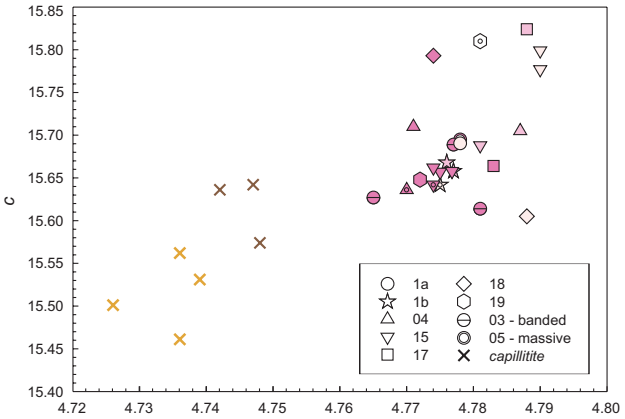

Fig. 13 Unit-cell parameters of the rhodochrosite samples from Capillitas. The filled symbols represent the different stalactitic samples, with the different pink tonalities trying to match the colorations described in Tab. 2. The symbols with a small circle inside correspond to data from the inner band in the stalactites. The white symbols with a horizontal line inside denote the banded rhodochrosite samples, while the circular, double border symbol corresponds to the massive rhodochrosite. The light brown and dark brown crosses represent the "capillitite" samples, coinciding with the variations in their tonalities.

The different shades of the pink color of rhodochrosite reflect variations in its chemical composition. Where MnO is associated with small quantities of CaO, the rhodochrosite is deeper pink, but where MnO is partially replaced by FeO and CaO ± MgO, the colors become paler. The presence of significant amounts of ZnO (up to 14 wt. %) associated with FeO (up to 20 wt. %) and smaller amounts of CaO result in brown colors ("capillitite"), although even under these circumstances Mn^{+2} is invariably greater than 50 % of the total sum of the cations.

There is no systematic relation between the different shades of pink color and the dimensions of the parameters of the rhodochrosite unit cell. There is only a slight tendency toward smaller values in dimensions associated with the more intense colorations. Where the color is brown ("capillitite"), the cell parameters are smaller. Also, the paler the brown colors, the smaller the dimensions of the cell parameters.

The stalactitic and non-stalactitic variants of rhodochrosite have a similar chemical composition and suggest a common source of mineralizing fluids prevailing at the end of the hydrothermal evolution, after the sulfide-rich polymetallic ore stage. Observations and data provided in this contribution suggest that the stalactites were possibly formed toward the end of the last stage of mineralization of the 25 de Mayo vein, from low salinity (≤ 4 wt. % $NaCl_{eq.}$) hydrothermal fluids at about 150 °C, just after the banded rhodochrosite was deposited, by infiltration of an epithermal aqueous liquid, oversaturated with Mn and bicarbonate, into a transiently vapor-filled, isolated cavity.

Acknowledgments. This study was made possible by the Argentinian support of CONICET through PIP 112-20120100554-CO, and PIP 112-20200101489-CO grants. The first author is very grateful to Todd Solberg for his dedicated training and helps in obtaining the microprobe data, Frank Hawthorne for the X-ray diffraction access, and Neil Ball for his help obtaining the X-ray data. The authors are also very grateful for the constructive reviews of Christoph A. Heinrich and Robert F. Martin. Finally, the editorial handling and comments of the Handling Editor Jiří Sejkora and the Editor-in-Chief Jakub Plášil are much appreciated.

References

Andrieux C (1965) Morphogenèse des helictites monocristallines. B Soc Franc Miner Crst, 88: 163–171

Angelelli V, Rayces EC (1946) Estudio geológico-minero del distrito cuprífero Capillitas, departamento Andalgalá, Provincia de Catamarca. Dirección General de Fabricaciones Militares. Unpublished report. Buenos Aires

Angelelli V, Schalamuk I, Cagnoni J (1974) La rodocrosita del yacimiento cuprífero de Capillitas, dpto. Andalgalá, prov. de Catamarca, República Argentina. Rev Asoc Geol Argent 29: 105–127

Appleman DE, Evans NT Jr. (1973) Job 9214: indexing and least- squares refinement of powder diffraction data. U.S. Geological Survey, Computer Contribution 20 (NTIS Doc. PB2- 16188)

Barton, PB Jr, Campbell, WR (1994) Occurrence, origin, and significance of stalactites in ore deposits. Eos, Trans Amer Geophys Un 75(16): 69 (abstract)

Bates, RL, Jackson JA (1980) Glossary of geology. Second Edition. American Geological Institute, Falls Church, VA, USA, pp 1–749

Behnke RE (2016) Trapiche rhodochrosite. Gems Gemol 52: 323

Brodtkorb A, Brodtkorb M (1979) Rhodochrosit aus Argentinien. Lapis 4/H 10 S: 19–22

Campbell WR, Barton PB Jr (1996) Occurrence and significance of stalactites within the epithermal deposit at Creede, Colorado. Canad Mineral 34:905–930

Cunningham CG, Aparicio NH, Murillo SF, Jiménez CN, Lizeca BJL, McKee EH, Ericksen GE, Tavera VF (1994) Relationship between the Porco, Bolivia, Ag-ZnPb-Sn deposit and the Porco caldera. Econ Geol 89: 1833–1841

Dolley CS (1886) On the helictites of Luray Cave. Proc Acad natur Sci, Philadelphia: 351–352

Effenberger H, Mereiter K, Zemann J (1981) Crystal structure refinements of magnesite, calcite, rhodochrosite, siderite, smithsonite, and dolomite, with discussion of some aspects of the stereochemistry of calcite type carbonates. Z Kristallogr 156: 233–243

Frisia S (2019) Stalactites and stalagmites. In: White W, Culver DC, Pipan T (eds) Encyclopedia of Caves, 3rd. Edition. Academic Press-Elsevier, Cambridge, MA, pp 1041–1048

Frisia S, Borsato A, Fairchild IJ, McDermott F, Selmo EM (2002) Aragonite-calcite relationships in speleothems (Grotte de Clamouse, France): Environment, fabrics, and carbonate geochemistry. J Sediment Res 72: 687–699

Galloni EE (1950) Capillitite - Crystal structure of Fe–Zn-rhodochrosite. Amer Miner 35: 562–570

Goldschmidt JR, Graf DL (1957) The system CaO–MnO–CO_2: solid solution and decomposition relations. Geochim Cosmochim Acta 11: 310–334

Goto M (1958) Stalactite from the Ezobanryu Stalactite Gorotto, Tōma-mura, Hokkaido. J Mineral Soc Japan 3: 557–564

Graf DL (1961) Crystallographic tables for the rhombohedral carbonates. Amer Miner 46: 1283–1316

Huff LC (1940) Artificial helictites and gypsum flowers. J Geol 48: 641–659

Kojima S, Sugaki A (1983) On the rhodochrosite stalagmite from the Oe Mine, Hokkaido, Japan. J Jap Assoc Mineralogists Petrologists Econ Geologists 78: 491–496

Lieber W (2000) Einmalige Tropfsteinbildungen aus Argentinien: Rhodochrosit-Stalaktiten. Lapis 25: 13–20

Maltsev VA (1998) Stalactites with "internal" and "external" feeding. Proc Univ Bristol Speleol Soc 21: 149–158

Márquez-Zavalía MF (1988) Mineralogía y génesis del yacimiento Capillitas (Catamarca, República Argentina). PhD thesis. Universidad Nacional de Salta, pp 1–284

Márquez-Zavalía MF (1999) El yacimiento Capillitas, provincia de Catamarca. In: Zappettini EO (ed) Recursos Minerales de la República Argentina. Anales SEGEMAR 35, Buenos Aires, pp 1643–1652

Márquez-Zavalía MF (2008) La rodocrosita de Mina Capillitas "Piedra" Nacional Argentina – Rosa del Inca. In: CSIGA (ed) Sitios de Interés Geológico de la República Argentina. Instituto de Geología y Recursos Minerales. Servicio Geológico Minero Argentino – Anales SEGEMAR 46, Buenos Aires, pp 85–98

Márquez-Zavalía MF, Craig JR (2004) Telluride and precious metal mineralization at Mina Capillitas, northwestern Argentina. Neu Jb Mineral Mh 2004: 176–192

Márquez-Zavalía MF, Heinrich CA (2016) Fluid evolution in a volcanic-hosted epithermal carbonate–base-metal–gold vein system: Alto de la Blenda, Farallón Negro, Argentina. Miner Depos 51: 873–902

Márquez-Zavalía MF, Galliski MA, Drábek M, Vymazalová A, Watanabe Y, Murakami H, Bernhardt H-J (2014) Ishiharaite, (Cu,Ga,Fe,In,Zn)S, a new mineral from Capillitas Mine, northwestern Argentina. Canad Mineral 52: 969–980

Márquez-Zavalía MF, Vymazalová A, Galliski MA, Watanabe Y, Murakami H (2020). Indium-bearing paragenesis from the Nueva Esperanza and Restauradora veins, Capillitas mine, Argentina. J Geosci 65: 95–109

Moore GW (1954) The origin of helictites. Natl Speleol Soc Occasional Papers 1: 3–16

Moore GW (1962) The growth of stalactites. Bull Natl Speleol Soc 24: 95–106

Onuk P, Dietzel M, Hauzenberger CA (2014) Formation of helictite in the cave Dragon Belly (Sardinia,Italy) – Microstructure and incorporation of Mg, Sr, and Ba. Chem Erde-Geochem 74: 443–452

Pouchou JL, Pichoir F (1985) "PAP*"* (ϕρZ) correction procedure for improved quantitative microanalysis. In: Armstrong JT (ed) Microbeam analysis. San Francisco Press, San Francisco, pp 104–106

Putz H, Paar WH, Topa D (2009) A contribution to the knowledge of the mineralization at mina Capillitas, Catamarca. Rev Asoc Geol Argent 64: 514–524

Radice MM (1949) Contribución al conocimiento mineralógico de la rodocrosita de yacimientos Argentinos. Rev Museo La Plata - Geol 4: 247–319

Shaub BM (1972) Rhodochrosite: the ornamental banded material from Argentina. Mineral Digest 4: 46–56

Swanson HE, Gilfrich NT, Cook MI (1957) Standard X-ray diffraction powder patterns. U. S. Natl Bureau Stand Circ 539: 7